

Heat Treatment Effect on Magnetic Microstructure of $\text{Fe}_{73.9}\text{Cu}_1\text{Nb}_3\text{Si}_{13.2}\text{B}_{8.9}$ Thin Films

Evgeniya Mikhailitsyna^{1,*}, *Ivan Zakharchuk*², *Ekaterina Soboleva*², *Pavel Geydt*², *Vasiliy Kataev*¹, *Vladimir Lepalovskij*¹, and *Erkki Lähderanta*²

¹Ural Federal University, Department of Solid State Magnetism, 620002 Ekaterinburg, Russia

²Lappeenranta University of Technology, School of Engineering Science, 53851 Lappeenranta, Finland

Abstract. $\text{Fe}_{73.9}\text{Cu}_1\text{Nb}_3\text{Si}_{13.2}\text{B}_{8.9}$ (Finemet) thin films were deposited on the glass substrates by means of radio frequency sputtering. The films thickness was varied from 10 to 200 nm. Heat treatment at temperatures of 350, 400 and 450 °C were performed for 30 minutes in order to control thin film structural state. The X-ray powder diffractometry revealed that the crystallization of α -FeSi nanograins took place only at 450 °C whilst the other samples stayed in the amorphous state. Relation between the structure and magnetic properties of the films was discussed in the framework of random magnetic anisotropy model and the concept of stochastic magnetic domains. The latter was investigated using magnetic force microscopy (MFM). MFM data showed formation of such magnetic domains only in samples thermally treated at 450 °C. There was a tendency of the magnetic domain size reduction with the thickness decrease.

1 Introduction

Nanocrystalline $\text{Fe}_{73.9}\text{Cu}_1\text{Nb}_3\text{Si}_{13.2}\text{B}_{8.9}$ alloy that is well known as Finemet retains a high scientific and technological interest due to its excellent magnetic properties among the soft magnetic materials [1-3]. Low coercivity and both high saturation magnetization and permeability determines a wide range of its applications as functional materials in power transformers, microwave devices, magnetic sensors and other [4-6]. These properties are caused by special microstructure of the alloy, which is characterized by randomly oriented ultrafine bcc α -FeSi grains uniformly dispersed in a residual Fe-Nb-B amorphous matrix. Macroscopic properties of Finemet alloy are closely related to the microscopic structural and magnetic parameters of the material such as grain size, saturation magnetization, magnetic anisotropy constant and exchange parameter. This relationship has been successfully described within the framework of random magnetic anisotropy model (RAM) [7].

In this report, we present a study of magnetic microstructure of $\text{Fe}_{73.9}\text{Cu}_1\text{Nb}_3\text{Si}_{13.2}\text{B}_{8.9}$ thin films depending on temperature of heat treatments and film thicknesses.

2 Experiment

2.1 Preparation of samples

Thin films were prepared by means of radio frequency ion-plasma sputtering of $\text{Fe}_{73.9}\text{Cu}_1\text{Nb}_3\text{Si}_{13.2}\text{B}_{8.9}$ target

onto a Wilmad glass substrates. The deposition was carried out in the presence of technical magnetic field of 100 Oe oriented parallel to the substrate. For all samples the achieved base pressure was of 10^{-6} Torr and the 99.987% Ar process pressure was of 10^{-3} Torr. The substrate temperature did not exceed 40-50 °C during the deposition. The structural state was controlled by a heat treatment. The samples were annealed at the pressure not worse than 10^{-3} Torr and at temperatures of 350, 400 and 450 °C for 30 min. Magnetic field was also applied during the heat treatments in the same direction as at depositions.

The thin films thicknesses of 10, 50, 100 and 200 nm were verified by means of Dektak 150 Stylus Profilometer.

2.2 Study techniques

Microstructure of the samples were identified using the Bruker D8 Advance X-Ray diffractometer operating at 40 kV and 40 mA, in theta-2theta configuration, and secondary monochromator with Cu-K_α radiation ($\lambda = 1.5418 \text{ \AA}$).

The atomic force (AFM) and magnetic force (MFM) microscopies were obtained using the Scanning Probe Microscope Bruker Multimode 8. The MFM mode of measurements is based on two-pass scanning technique. The sample topology was recording in the tapping mode during the first pass. During the second one, magnetic phase contrast was measuring in the lift mode that means scanning with a constant distance between the probe and the sample surface (typically of about 80-100 nm). The scans were performed in the presence of external

* Corresponding author: evgenia.mihalitsyna@urfu.ru

magnetic field ($H \sim 180$ Oe) directed out-of-plane to the sample surface. The scan area was $10 \times 10 \mu\text{m}^2$ (resolution 512×512 pixels) and the scan rate was 0.150 Hz. Tip with approximate radius of 40 nm, magnetic CoCr coating, and spring constant of 5 N/m was used in experiments.

The in-plane hysteresis loops in both easy magnetization axis (EA) and hard magnetization one (HA) were measured at room temperature by Evico magnetics GmbH magneto-optical Kerr effect (MOKE) microscope using an overview mode.

3 Results and discussion

Room temperature X-Ray diffraction (XRD) patterns of the as-prepared and annealed samples were measured in the angle range of $10^\circ \leq 2\theta \leq 120^\circ$. Large halo in the small angles range was corresponded to the signal from the substrate. As-prepared and annealed at 350 and 400 °C films were mainly in roentgen-amorphous state (Fig. 1, top picture). The presence of crystalline phase was identified in samples annealed at 450 °C. The broadened peak for an angle of order $2\theta=45^\circ$ in Fig. 1 (bottom picture) indicates that the phase α -FeSi is formed in the films [1,2]. The average size of nanocrystalline α -FeSi grains was estimated of 16 ± 6 nm using the Scherrer's formula for cubic particles.

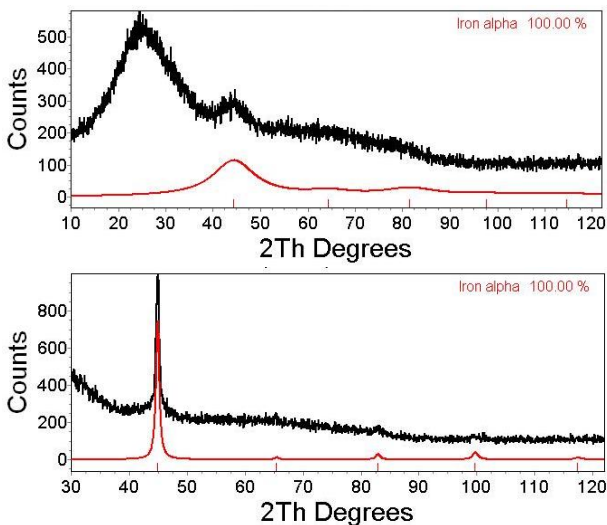


Fig. 1. XRD patterns of 200 nm films in the as-prepared state (top) and after the heat treatment at the temperature 450 °C for 30 min (bottom).

As can be seen from the joint consideration of the XRD data and hysteresis loops in Figs. 2a-2c the thin films before crystallization are characterized by a soft magnetic behavior with in-plane magnetic domains. Induced magnetic anisotropy is observed for the films in as-prepared state. Increase of the annealing temperature leads to decrease of the induced anisotropy field and its total disappearance for the film annealed at 450 °C (Fig. 2d). Assuming magnetoelastic nature of the induced anisotropy, decreasing of anisotropy field can be explained by the internal stresses relaxation.

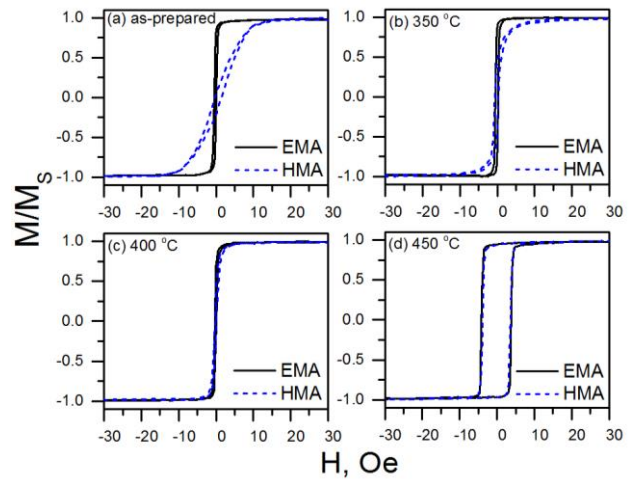


Fig. 2. MOKE hysteresis loops measured along easy and hard magnetization axes of the 200 nm films in the as-prepared state (a) and after the heat treatment at 350 (b), 400 (c) and 450 °C (d).

A surface topography of the 200 nm films annealed at 400 and 450 °C are presented in Figs. 3a and 3c. As can be seen in Fig. 1 and Fig. 3c heat treatment at the temperature of 450 °C leads to the crystallization and formation of the grain-like structure on the film's surface. The grains size is about 60-90 nm in diameter and 7-10 nm in height. The result of AFM study shows that root mean square roughness increases approximately from 1.6 nm to 4.1 nm when the annealing temperature goes up.

The MFM image of the 200 nm thick film annealed at 450 °C shows appearance of magnetic contrast on the surface. A size of the uniform contrast regions is about of 300-600 nm in width and $10 \mu\text{m}$ in length (Fig. 3d). However, there is no visible magnetic contrast on the surface of the same thickness thin film annealed at 400 °C as shown in Fig. 3b.

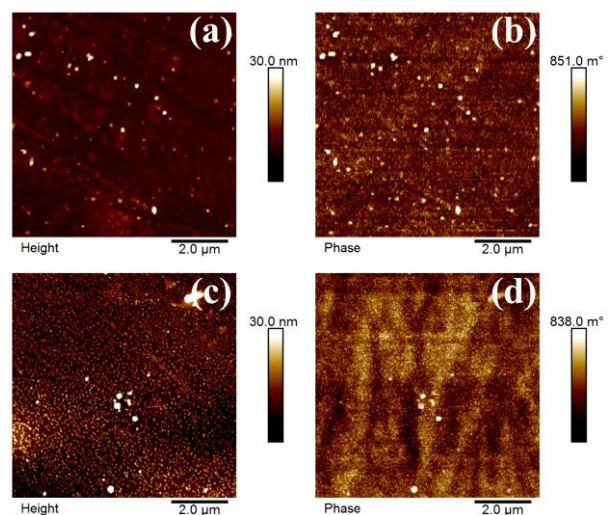


Fig. 3. AFM (a, c) and MFM (b, d) patterns of the 200 nm films after the annealing at 400 °C (a, b) and 450 °C (c, d).

The absence of magnetic contrast on the surface of 400 °C annealed film could be connected with a very

low coercivity of the film. So, a probe magnetic field could affect on a sample magnetic structure.

The areas of uniform contrast on the MFM images in Fig. 3d can be correlated with the extension of the magnetic correlation region. And the image as a whole can represent a stochastic magnetic domain structure. The change in color contrast will correspond to an inhomogeneous distribution of the magnetization.

As mentioned earlier, the heat treatment at 450 °C leads to crystallization. According to the assumption of random magnetic anisotropy model, easy magnetization axes of grains are randomly oriented. Due to strong exchange coupling (that needs small enough grain sizes $D \ll \sqrt{A/K}$, where A is an exchange stiffness constant and K is a local anisotropy constant) between grains, correlated magnetic microstructures are formed. Within these correlated regions averaging of local magnetic properties provides a decreased efficient anisotropy constant and, subsequently, low coercivity. It should be noted that the sample annealed at 450 °C has a markedly greater value of coercivity (Fig. 3d). The possible reason of it is a sufficiently large grain size for the effective averaging within the RAM framework, but it does not exclude the existence of stochastic domains.

Stochastic magnetic structure appears for all samples annealed at 450 °C. Consequently, a next step is to investigate the evolution of the domain structure with the film thickness. The surface topology and magnetic contrast images of the samples with the thicknesses of 10, 50, 100 and 200 nm are presented in Fig. 4. All samples demonstrate the presence of the grains on the film's surface as the result of crystallization process [8]. Here the size of the grains increases from 60-90 up to 300 nm with the thickness decreasing. Topography of very thin films can be affected the glass substrate characterized by prolonged irregularities. Also, thickness decreasing can restrict structural transformation in the direction perpendicular to the film plane.

It is clearly seen in MFM images in Fig. 4 the domains become thinner and almost disappear in the 10 nm film with the film thickness decreasing. Similar results were observed in Refs. [9-10] for FeSiB thin films.

Parameters of stochastic magnetic domains are defined by microscopic parameters such as exchange constant, saturation magnetization, local magnetic anisotropy constant and grain size. The influence of each parameter should be studied in details. One can only conclude that the decrease of thickness has an effect on the size of heterogeneous magnetic contrast regions. A dimensionality of magnetic correlations can decrease when film becomes thinner. As a result, efficiency of local anisotropy axes averaging deteriorates, that is directly connected with the stochastic domain size [11].

Moreover anisotropic form of the magnetic domains in MFM images of the film with thickness of 50, 100 and 200 nm should be mentioned despite the samples are completely isotropic after the heat treatment at 450 °C as shown in Fig. 2d.

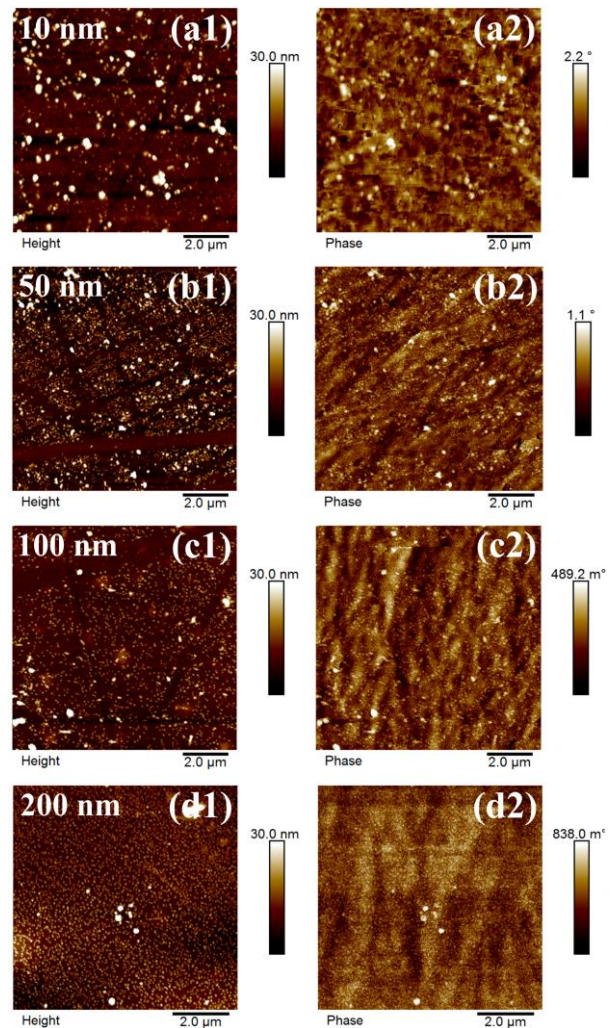


Fig. 4. AFM (a1-e1) and MFM (a2-e2) images of the films with thicknesses of 10 (a), 30 (b), 50 (c), 100 (d) and 200 nm (e) after the heat treatment at 450 °C.

4 Conclusion

To conclude, magnetic and morphology microstructure of Fe_{73.9}Cu₁Nb₃Si_{13.2}B_{8.9} thin films of various thickness were investigated using XRD, AFM, MFM, MOKE microscope, and SQUID magnetometer. It was found that the heat treatment leads to increase of surface roughness and size of grains on the surface. The MFM detected presence of magnetic contrast on the surface of the films annealed at 450 °C that could be interpreted as stochastic magnetic domains. The domain size decrease with the film thickness decreasing.

The research was supported by the Ministry of Education and Science of the Russian Federation Agreement no. 02.A03.21.0006 and project no. 3.6121.2017.

References

1. Y. Yoshizawa, S. Oguma, K. Yamaguchi, J. Appl. Phys. **64**, 6044 (1988)

2. Y. Yoshizawa, K. Yamaguchi, *Mater. Trans. JIM* **31**, 307 (1990)
3. K. Hono, A. Inoue, T. Sakurai, *Appl. Phys. Lett.* **58**, 2180 (1991)
4. J. Moulin, I. Shahosseini, F. Alves, F. Mazaleyrat, J. Micromech. Microeng. **21**, 074010 (2011)
5. V. Prida, P. Gorria, G. Kurlyandskaya, M. Sanchez, B. Hernando, M. Tejedor, *Nanotechnology* **14**, 231 (2003)
6. M. Vazquez, G. Kurlyandskaya, J. Garcia-Beneytez, J. Sinnecker, *IEEE Trans. Mag.* **35**, 3358 (1999)
7. G. Herzer, *Acta Mater.* **61**, 718 (2013)
8. E. Mikhailitsyna, V. Kataev, P. Geydt, V. Lepalovsky, E. Lähderanta, *Solid State Phenom.* **233–234**, 699 (2015)
9. M. Coisson, F. Vinai, P. Tiberto, F. Celegato, J. *Magn. Magn. Mater.* **321**, 806 (2009)
10. M. Coisson, F. Celegato, E. Olivetti, P. Tiberto, F. Vinai, M. Baricco, *J. Appl. Phys.* **104**, 033902 (2008)
11. R. S. Iskhakov, S. V. Komogortsev, *Phys. Met. Metallogr.* **112**, 666 (2011)